Solution Preparation of Two-Dimensional Covalently Linked Networks by Polymerization of 1,3,5-Tri(4-iodophenyl)benzene on Au(111)

Georg Eder,[†] Emily F. Smith,[‡] Izabela Cebula,[‡,§] Wolfgang M. Heckl,[†,∥] Peter H. Beton,[§,*] and Markus Lackinger[†,∥,*]

[†]TUM School of Education and Center for NanoScience (CeNS), Tech Univ Munich, Schellingstrasse 33, 80799 Munich, Germany, [‡]School of Chemistry and [§]School of Physics and Astronomy, University of Nottingham, University Park, Nottingham NG7 2RD, United Kingdom, and [∥]Deutsches Museum, Museumsinsel 1, 80538 Munich, Germany

ABSTRACT The polymerization of 1,3,5-tri(4-iodophenyl)-benzene (TIPB) on Au(111) through covalent aryl—aryl coupling is accomplished using a solution-based approach and investigated by scanning tunneling microscopy. Drop-casting of the TIPB monomer onto Au(111) at room temperature results in poorly ordered noncovalent arrangements of molecules and partial dehalogenation. However, drop-casting on a preheated Au(111) substrate yields various topologically distinct covalent aggregates and networks. Interestingly, some of these covalent nanostructures do not adsorb directly on the Au(111) surface, but are loosely bound to a disordered layer of a mixture of chemisorbed iodine and molecules, a conclusion that is drawn from STM data and supported by X-ray photoelectron spectroscopy. We argue that the gold surface becomes covered by a strongly chemisorbed iodine monolayer which eventually inhibits further polymerization.

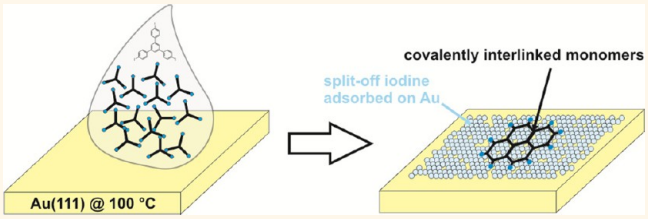

KEYWORDS: polymerization · liquid—solid · homolysis · halogenated monomer · STM · XPS · Au(111)

Over recent years the linking of small organic molecules on surfaces to form 1D and 2D polymeric structures has attracted great interest,[1−8] most lately due to the demonstration that this provides a route to nanostructured graphene with controlled dimensions.[9,10] A promising approach to generate 2D polymers is based on an Ullmann-type reaction, where halogenated monomers are covalently interlinked with the aid of a metal catalyst.[11] In this approach, the weakly bound halogen substituents are homolytically cleaved off and the resulting radicals recombine into covalent networks.[5,12−14] The network dimensionality and topology is thus determined by the halogen substitution pattern of the monomer. In the surface variant of the Ullmann reaction, the substrate serves as both the catalyst for homolysis and supporting template for the resulting network.

To date, this route is predominately pursued in ultrahigh vacuum (UHV) environments on coinage metal surfaces.[7,13,15,16] However, successful on-surface polymerization has already been demonstrated at the liquid—solid interface using alternative reaction strategies such as the Schiff base reaction[17] or boronic acid condensation,[18,19] which has been previously used for the synthesis of crystalline porous bulk materials, termed covalent organic frameworks.[20,21] Boronic acid condensation was also demonstrated on surfaces and yields well-ordered, two-dimensional covalent networks with domain sizes up to ∼50 nm, although the π-conjugation, obtainable through the Ullmann reaction, remains elusive for this approach. In addition, owing to the reversible nature of the employed condensation reactions, the resulting covalent networks only exhibit limited chemical stability.[22] Other approaches under ambient conditions encompass electrochemical epitaxial polymerization as well as light and local probe-induced polymerization.[6,23,24] Yet, these

* Address correspondence to markus@lackinger.org, peter.beton@nottingham.ac.uk.

Received for review July 31, 2012 and accepted March 10, 2013.

Published online March 11, 2013
10.1021/nn400337v

approaches remain restricted to specifically designed model systems. The development of a more general and flexible approach to the on-surface formation of more robust and functional 1D and 2D polymers motivates the transfer of the Ullmann-type reaction discussed above from UHV to a liquid environment. Initial attempts to achieve this goal have been limited to the formation of dimers and more extended structures have not yet been demonstrated.[25]

We have therefore studied the covalent linking of the monomer 1,3,5-tri(4-iodophenyl)benzene (TIPB) on Au(111). TIPB is a chemically stable triply iodinated organic building block that is composed of four phenyl rings and three terminating iodine atoms (the structure is shown in Figure 1a). Au(111) is chosen as a substrate because it is the best compromise between inertness against ambient contamination and sufficiently high catalytic activity for the dehalogenation reaction.[26] Furthermore, recent polymerization studies with the same compound on Au(111) under UHV conditions[27] facilitate a direct comparison between the two approaches and in addition with previous studies of 1,3,5-tri(4-bromophenyl)benzene (TBPB), the brominated analogue of TIPB.[12,14,25] As discussed above, previous studies of TBPB in a solution environment yielded only ordered arrangements of covalently interlinked dimers but very few higher oligomers and no larger covalent aggregates.[25] Consequently, in the present work we enhance the monomer reactivity by substitution of bromine with iodine, thereby taking advantage of the lower bond dissociation energy of the C–I bond and explore possibilities to form more extended covalent structures. Results of drop-cast deposition of the monomer onto the substrate held at room temperature are compared with results obtained on substrates that were preheated to 100 °C. The high resolution structural characterization by STM is augmented by chemical characterization using X-ray photoelectron spectroscopy (XPS).

RESULTS AND DISCUSSION

In Figure 1a,b we show STM images of the surface acquired following room temperature deposition of TIPB dissolved in nonanoic acid (9A) from solutions with different concentrations. These images were acquired while the sample was still covered with a liquid film with the STM tip immersed into solution. For the lower concentration (0.02 mmol/L; Figure 1a), the images show predominantly monolayer coverage with some short-range ordering. The angle between differently oriented domains is a multiple of 30° and, thus, indicates formation of nonequivalent rotational domains (see Figure 1a and Supporting Information). Higher resolution images (Figure 1a, lower middle inset) show trigonal features in a quasi-close packed arrangement. These features are highly reminiscent of that recently reported for the brominated analogue

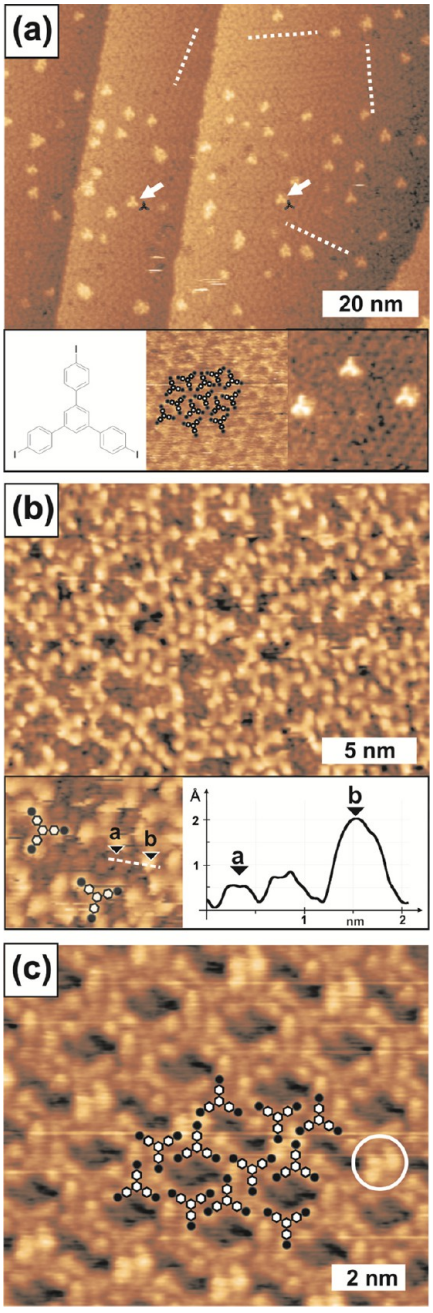

Figure 1. STM topographs of TIPB on (a, b) Au(111) and (c) graphite(0001). All images were acquired in 9A solution. (a) Obtained with a concentration of c = 0.02 mmol/L. The STM image represents small domains of ordered TIPB molecules, where individual adsorbed TIPB molecules in the second layer are highlighted by white arrows. White dotted lines indicate orientations of first layer domains. The insets depict the chemical structures of TIPB, a domain of TIPB molecules directly adsorbed on the Au(111) surface, and a zoom-in of second layer TIPB. (b) Obtained with a concentration of c = 0.04 mmol/L, resulting in an increased coverage of the second layer. The inset shows a zoom-in, where some features of the first layer are still visible. The terminating iodine atoms are highlighted by white dots. The line-profile shows a clear dip in the monolayer features, confirming the formation of a bilayer system. (c) Obtained with saturated solution on graphite. A molecular overlay indicates the tentative arrangement within the well-ordered monolayer. STM tunneling parameters: (a) I_t = 12 pA, U_t = 0.26 V; (b) I_t = 61 pA, U_t = −0.62 V; (c) I_t = 46 pA, U_t = 0.74 V.

TBPB both in UHV and in layers formed by drop-casting ethanolic solutions.[12,14,25] We attribute these features to intact TIPB monomers. Also present in Figure 1a are isolated bright features (examples are marked by white arrows) that, as shown in the lower right inset, have a clear 3-fold symmetry. These are identified as second layer TIPB molecules and the experimentally measured vertex−vertex dimensions of 1.4 ± 0.1 nm are in excellent agreement with the geometry optimized structure of intact TIPB molecules with an iodine−iodine distance of approximately 1.4 nm.

For higher concentrations (0.04 mmol/L; Figure 1b), we observe a higher density of TIPB in the second layer with an apparent height of ∼0.13 nm (see profile inset) with respect to the first monolayer. While there is no long-range ordering in the second layer, the image in Figure 1b shows features with a clear bright protrusion at each molecular lobe which are assigned to the peripheral iodine atoms of single molecules. It is noteworthy that, for self-assembly at the liquid−solid interface, stable adsorption in the second layer is rather uncommon and has only been observed in very few systems.[28]

Although highly disordered, it is interesting to compare the relative placement of molecular pairs in the second layer with those in the first layer and also in TIPB monolayers adsorbed on graphite. For this reason we show in Figure 1c a representative STM image of a self-assembled monolayer of TIPB on graphite using 9A as a solvent. This structure is well-ordered and densely packed. The molecular overlay indicates the structural model and the bright protrusions marked by the white circles are identified as cyclic arrangements of four iodine atoms that stabilize the structure by halogen−halogen interactions.[29,30] For adsorption of TIPB on the second layer on Au(111), we observe similar local arrangements where three or four iodine atoms meet. Another common junction observed in Figure 1a, two trigonal features meeting end-to-end, is also observed in the second layer; see for example the molecular pair at the bottom of the right inset to Figure 1b. In addition there are molecular junctions on the TIPB monolayer on graphite where an iodine atom from one molecule sits between two iodine atoms on a neighboring molecule (see molecular pair at the bottom center of the overlaid schematic of Figure 1c). There are many examples of this motif in Figure 1b. Overall we suggest that the second layer TIPB may be considered as a disordered version of the nanoporous monolayer physisorbed on graphite. Note also in Figure 1b the molecular arrangement forms partially completed nanopores with comparable dimensions and, in some cases, shapes to those formed on graphite. From the above discussion it is thus concluded that at room temperature the second layer TIPB molecules remain intact on the surface and the halogen substituents are not split-off. We are not able to resolve individual molecules in the underlying layer at this concentration.

In order to promote covalent interlinking, the Au(111) substrate was preheated to 100 °C on a hot plate under ambient conditions and 5 μL of TIPB solution with a notably higher concentration of $c = 0.80$ mmol/L was drop-cast on the surface. The sample remained on the hot plate for ∼120 s and was then allowed to cool down under ambient conditions. After this procedure, the solvent was almost fully evaporated. The sample was immediately characterized by STM and various aggregates such as 1D chains, open rings, closed pentagons, hexagons, heptagons, as well as more extended and irregular networks are clearly recognizable. Representative examples are depicted in Figure 2a. An analysis of the separation of the 3-fold vertices within this network is consistent with the formation of covalent aryl−aryl bonds. The experimental value, 1.3 ± 0.1 nm was found to be common in all types of aggregates. This value is in excellent agreement with both the figure calculated using density functional theory[27] and UHV experiments on topologically similar covalent networks,[12] verifying covalent bond formation.

The domain size observed in Figure 2a is comparable with those formed in UHV, but the total area covered by the covalent networks is smaller.[27] Moreover the formation of domains with up to 25 molecules with lateral dimensions up to 10 nm represents a major step forward from previous liquid studies, where no closed polygons were formed.

A more detailed analysis of the covalent structures reveals that several molecular lobes that do not take part in the covalent interlinks are often still terminated by iodine. Incomplete dehalogenation might be a possible reason for premature termination of the polymerization, hence mostly resulting in oligomers of finite size. Also the STM images predominantly show aggregates on substrate terraces, suggesting that the reaction is not restricted to step-edges. Changing the solvent to a shorter fatty acid, namely, heptanoic acid, while applying the same preparation protocol yielded similar results (see Supporting Information).

The catalytic role of the metallic Au(111) substrate in iodine homolysis was confirmed through control experiments with similar deposition protocols using as substrates both graphite(0001) and Au(111) intentionally terminated with iodine. The latter sample was prepared by immersing a freshly flame annealed Au(111) sample into 3 mM aqueous KI solution for 180 s and subsequent rinsing with ethanol (*cf.* Supporting Information). Drop-casting of TIPB solution on these substrates preheated to 100 °C did not yield any covalent structures. Both surfaces proved inactive for iodine homolysis, confirming the important catalytic contribution of the bare Au(111) surface, and,

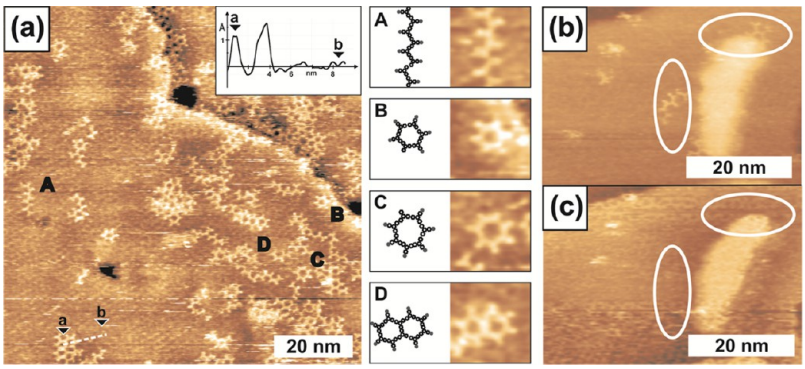

Figure 2. (a) STM topograph of covalently interlinked structures from TIPB polymerization; the sample was prepared by deposition of 5 μL of TIPB solution in 9A (c = 0.80 mmol/L) onto Au(111) held at 100 °C and cooling down after 120 s. The STM image depicts covalent aggregates on top of a first monolayer; close-ups (A–D) of frequently encountered covalent aggregates are presented on the middle: (A) one-dimensional chains, (B) closed hexagons, (C) closed heptagons, and (D) more extended structures as merged rings; besides that, more extended irregular structures and open rings were frequently observed. (b, c) Consecutively recorded STM images revealing the detachment of covalent aggregates. As highlighted by white circles covalently interlinked aggregates that were still present in (b) have disappeared in (c). STM tunneling parameters: (a) I_t = 63 pA, U_t = −0.752 V; (b, c) I_t = 58 pA, U_t = −0.624 V.

moreover, showing that Au(111) becomes catalytically inactive by iodine adsorption.

For deposition onto bare Au(111) held at 100 °C, some of the covalent aggregates are not directly adsorbed on the metal surface, but on top of an intermediate monolayer. This conclusion is supported by the STM data, where covalent aggregates appear ∼0.10–0.20 nm higher than the first monolayer. On the contrary, covalent structures obtained in UHV experiments are directly supported on metal surfaces and appear lower than the split-off iodine atoms in STM images.[27] The STM appearance of the covalent structures in Figure 2 directly compares to those obtained in polymerization studies carried out previously on iodine-terminated Au(111).[17,31,32] Furthermore, in UHV, the contrast within closed pores of covalent networks either appears significantly lower than the polymers or the halogens, that is, indicating empty pores, or with inhomogenous features due to entrapment of molecules or atoms within the pores, whereas in Figure 2a the pore interiors appear with uniform contrast and the same height as the surrounding. In addition, the covalent aggregates are rather weakly adsorbed, as shown by the occasional observation of their detachment and displacement during STM imaging (compare Figure 2b and c).

Additional STM experiments were carried out in order to investigate the origin of this monolayer. Figure 3 shows an STM topograph acquired after the sample was annealed at 100 °C for 120 min. We interpret this image as showing adsorbed iodine on Au(111) intermingled with an array of dark pores. Higher magnification images show a more detailed view of the directly adsorbed first monolayer; see close-up in Figure 3c. Examples for frequently observed pairs of spherical features with 0.5 nm spacing are highlighted by pairs of blue arrows. This distance cannot be matched with any intramolecular distance of TIPB or its networks. In addition, the 2D FFT of this STM image indicates hexagonal symmetry. Interestingly, there is a clearly visible hexagonally arranged group of inner spots (marked by the dashed circle in Figure 3c), but also faint outer spots can be recognized (two spots are exemplarily marked by arrows). The inner spots correspond to a period of ∼1.7 nm, indicating both a more or less regular spacing and a nonrandom azimuthal orientation of the dark pores. The outer spots correspond to a period of ∼0.5 nm and can be separated into two groups of hexagonally arranged spots that are rotated by ∼16° with respect to each other. The period is similar to the nearest neighbor iodine–iodine distance in the various coverage-dependent superstructures found for pure iodine monolayers on Au(111).[33] The presence of chemisorbed iodine within the first monolayer is further substantiated by XPS data (*vide infra*). Based on these experiments, we propose that iodine from cleaved bonds adsorbs on, and poisons the Au(111) surface thus inhibiting any further catalytically supported iodine homolysis. We further propose that chemisorbed iodine also displaces partially formed covalent networks from the surface leading to weak adsorption in a second layer.

XPS experiments were performed in order to confirm the presence of chemisorbed iodine on the gold surface. Different sample preparations were compared: drop-casting TIPB in 9A solutions with two different concentrations (0.02 and 0.80 mmol/L) onto Au(111) either held at room temperature or heated to 100 °C. First, 5 μL solution were applied to a freshly flame annealed Au(111), then after 2 h, where the surfaces were held at the respective temperature, the samples were rinsed with pure ethanol and immediately transferred to the XPS chamber. No further annealing or further treatment was carried out before the measurement.

Spectra highlighting the binding energy region of the I(3d) core levels are depicted in Figure 4. In the XPS

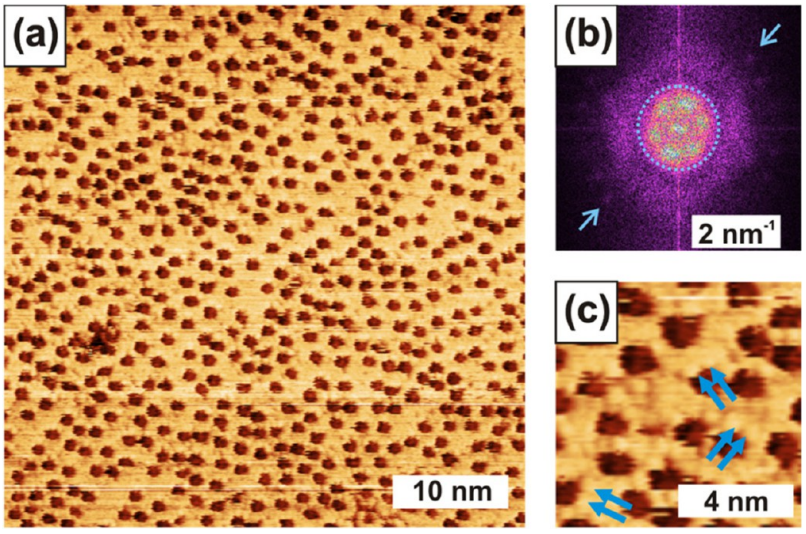

Figure 3. (a) STM topograph obtained after drop-casting 0.80 mmol/L TIPB solution in 9A onto Au(111) at a surface temperature of 100 °C and extended heating for 120 min (b) corresponding FFT to (a); the inner hexagonally arranged group of diffuse spots (marked by the dashed circle) corresponds to a real space distance of ~1.7 nm and indicates a regular spacing and a preferred azimuthal orientation of the dark pores. The outer faint spots (examples marked by arrows) correspond to a real space distance of ~0.5 nm. The outer spots consist of two hexagonally arranged groups that are rotated by 16° with respect to each other. (c) Close-up to (a); the pairs of blue arrows highlight 0.5 nm spaced spherical features that are assigned to nearest neighbor chemisorbed iodine atoms. STM tunneling parameters: I_t = 35 pA, U_t = −0.359 V.

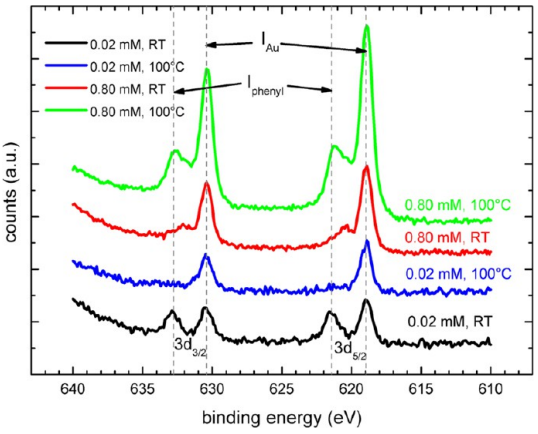

Figure 4. XPS measurements of TIPB deposited onto Au(111) from 9A solution under ambient conditions. Two different concentrations, 0.02 and 0.80 mmol/L, were applied and the Au(111) surface was either held at room temperature or preheated to 100 °C. After maintaining the respective surface temperature for 2 h, the samples were rinsed with pure ethanol. The curves are vertical offset for clarity, but were not normalized otherwise. All spectra were acquired under similar conditions, thus intensities directly correspond to iodine concentrations. The spectra show I $3d_{3/2}$ and $3d_{5/2}$ spin−orbit doublets and typical binding energies for the chemically distinct iodine species I_{phenyl} and I_{Au} are indicated by the vertical dashed lines, respectively.

data of room temperature deposited TIPB with 0.02 mmol/L (black curve in Figure 4) four peaks can be discerned that correspond to spin−orbit doublets of two chemically distinct iodine species. The spin−orbit doublet at binding energies of 621.4 eV (I-$3d_{5/2}$) and 632.8 eV (I-$3d_{3/2}$) arises from unreacted TIPB with binding energies comparable to similar iodinated aromatic compounds.[34] This iodine species is referred to as I_{phenyl} in the following. The additional spin−orbit doublet at 619.0 eV (I-$3d_{5/2}$) and 630.5 eV (I-$3d_{3/2}$) is attributed to iodine chemisorbed on Au(111) as identical binding energies were obtained in XPS control measurements on iodine terminated Au(111) surfaces (cf. Supporting Information). These binding energies are also consistent with XPS spectra for iodine adsorbed on other coinage metals, where the characteristic I-$3d_{5/2}$ peaks were found at 619.0 eV for Cu−I and 619.4 eV for Ag−I, respectively.[35] Chemisorbed iodine is referred to as I_{Au} in the following. The presence of I_{Au} for room temperature drop-cast samples indicates that spontaneous dehalogenation of TIPB molecules already occurs without additional thermal activation. However, drop-casting a low concentration solution on Au(111) held at 100 °C (blue curve in Figure 4), leads to the disappearance of I_{phenyl}. This indicates amounts of unreacted or partially reacted TIPB below the detection limit, while the I_{Au} peak increases in intensity. The onset of dehalogenation at room temperature is an obvious limitation for self-assembly of well-ordered TIBP structures on Au(111).

The XPS measurements obtained after room temperature drop-casting 0.80 mmol/L solution appear different (red curve in Figure 4). While I_{Au} is clearly present, I_{phenyl} is only visible as a small shoulder, indicating an enhanced dehalogenation rate at room temperature for higher concentrations. Interestingly, I_{Au} increases for the high concentration, 100 °C drop-cast samples (green curve in Figure 4), but also I_{phenyl} becomes slightly more prominent. This confirms larger amounts of chemisorbed iodine when solutions with higher solute concentration are applied and

implies that for low concentration the Au(111) surface is not saturated with iodine. Enhancement of I_{phenyl} can be explained by the STM data, which show that for higher concentrations, the covalent aggregates become larger and, accordingly, less soluble. These data provide explicit support for our interpretation of the STM image shown in Figure 3.

The onset of the reaction at room temperature is in accordance with UHV experiments on 1,3,5-triiodobenzene on Au(111), where covalently interlinked aggregates were likewise already observed at room temperature.[27] In general, the Au(111) surface is known to act as a catalyst for the homolysis of carbon–halogen bonds.[8,9,36] However, in contrast to iodine homolysis, the cleavage of bromine substituents on Au(111) requires thermal activation, as demonstrated in UHV and ambient conditions at temperatures of 140 to 180 °C[12] and 200 °C,[25] respectively. The reactivity difference between iodinated *versus* brominated monomers can be rationalized by pronounced differences in the carbon–halogen bond dissociation energy, with C–Br bonds (3.49 eV in bromobenzene) being significantly stronger than the C–I bonds (2.84 eV in iodobenzene).[37] Whereas, according to a systematic DFT study, the binding energy of bromine on Au(111) amounts to 2.26 eV and is even slightly higher than that of iodine of 2.14 eV.[38] In any case, halogens strongly chemisorb on Au(111), as further expressed by a high desorption temperature. Syomin *et al.* reported an I_2 desorption peak maximum at 450 °C for temperature-programmed desorption after C_6H_5I exposure on gold.[36]

Based on the experimental STM and XPS results, we propose the following reaction scheme. Even for room temperature deposition of TIPB molecules, initial dehalogenation spontaneously occurs, while the reaction rate becomes significantly enhanced at 100 °C and for higher concentrations. The catalytic activity of Au(111) is required for the activation of polymerization, as shown by control experiments on intentionally iodine-terminated Au(111) surfaces and graphite (0001). Following dehalogenation, radicals recombine and form new covalent aryl–aryl bonds. However, extended covalent aggregates are not observed after room temperature deposition, possibly due to the limited room temperature mobility of the radicals, and there is clear evidence that unreacted monomers remain on the surface. Drop-casting onto heated substrates results in covalent aggregates that are adsorbed on a monolayer of chemisorbed I and unreacted or partially reacted molecules. The presence of split-off iodine atoms is unambiguously confirmed by XPS experiments. Owing to the progressive adsorption of split-off iodine atoms onto the Au(111) surface the substrate becomes catalytically inactive for iodine homolysis suppressing further coupling reactions. The chemisorbed iodine layer not only poisons the substrate, but also displaces covalent aggregates into the second layer, where they are only adsorbed weakly.

CONCLUSION

It has been shown that the polymerization of the triply iodinated monomer TIPB can be initiated by deposition from solution onto a preheated Au(111) surface. In contrast to similar experiments under ambient conditions with TBPB, the brominated analogue of TIPB, more extended covalent structures that consist of up to 25 monomeric units were obtained, while the brominated monomer yielded only dimers, consistent with the enhanced reactivity of iodinated precursors for the proposed polymerization reaction. Interestingly, most of the covalent structures were found on top of a chemisorbed monolayer. The presence of the covalent aggregates in a second layer is unique to the solution approach and has not been observed in UHV experiments. The observed displacement and detachment during STM imaging indicates a rather weak interaction with the underlying first monolayer acting as a buffer to Au(111). This observation is particularly interesting for the development of strategies to transfer these covalent aggregates from the catalytically active surfaces that are indispensable for their synthesis to alternative surfaces that are more promising in terms of applications.

Overall, the increased reactivity of iodinated compounds make them more promising candidates than their brominated analogues for polymerization under ambient conditions and permits the use of relatively inert surfaces such as gold. Our results indicate that, to further improve the order and size of the covalent networks, it will be necessary to reduce the effect of the iodine-induced deactivation of the catalytic surface. This raises several interesting scientific issues and there are several possible strategies, for example, methodologies for the partial removal of iodine through the introduction of other reagents and through the synthesis of modified monomers, which adsorb more strongly on the gold surface. The results presented here strongly motivate such studies.

MATERIALS AND METHODS

The STM experiments were conducted with an Agilent Technologies 4500 PicoPlus STM using a PicoScan controller. Commercially supplied (111) terminated gold films on mica (Georg Albert, Physical Vapor Deposition) were used as substrates and prepared by flame-annealing prior to the experiments. STM tips were mechanically cut from a platinum/iridium (80/20) wire. The atomic lattices of graphite(0001) and Au(111) were used for lateral calibration of the STM, and experimental distances were derived with an accuracy of <0.1 nm.

The monomer 1,3,5-tri(4-iodophenyl)benzene (TIPB, Sigma Aldrich) was used as supplied and dissolved in nonanoic acid (9A, Sigma Aldrich) and heptanoic acid (7A, Sigma Aldrich). During the deposition, the substrate was either held at room temperature or preheated to 100 °C on a hot plate under atmospheric conditions. Samples for XPS were prepared under ambient conditions, with the substrate either held at room temperature or preheated to 100 °C. The samples were kept at the respective temperature for 2 h, rinsed with pure ethanol, and then transferred into the XPS chamber. A Kratos AXIS ULTRA DLD instrument with a monochromated Al Kα X-ray source (1486.6 eV) was used and operated at 10 mA emission current and 12 kV anode potential. The lens mode used was hybrid-slot and pass energies 80 and 20 eV were used for the wide and high resolution scans, respectively. Spectra were acquired at room temperature.

Conflict of Interest: The authors declare no competing financial interest.

Acknowledgment. P.H.B. acknowledges useful discussions with Prof. Neil Champness (School of Chemistry, University of Nottingham) and funding was provided by the UK Engineering and Physical Sciences Research Council. G.E. is particularly grateful for financial support by the Hanns-Seidel-Stiftung and Kurt Fordan Förderverein für herausragende Begabung e.V. M.L. acknowledges funding by the DFG (LA1842/4) and Nanosystems-Initiative-Munich (NIM). We would like to thank Jürgen Dienstmaier for his help with the STM control experiments.

Supporting Information Available: Additional STM images of room temperature adsorption of TIPB, solvent influence, and iodine-terminated Au(111) surface. This material is available free of charge *via* the Internet at http://pubs.acs.org.

REFERENCES AND NOTES

1. Treier, M.; Fasel, R.; Champness, N. R.; Argent, S.; Richardson, N. V. Molecular Imaging of Polyimide Formation. *Phys. Chem. Chem. Phys.* **2009**, *11*, 1209–1214.
2. Jensen, S.; Greenwood, J.; Früchtl, H. A.; Baddeley, C. J. STM Investigation on the Formation of Oligoamides on Au{111} by Surface-Confined Reactions of Melamine with Trimesoyl Chloride. *J. Phys. Chem. C* **2011**, *115*, 8630–8636.
3. Treier, M.; Richardson, N. V.; Fasel, R. Fabrication of Surface-Supported Low-Dimensional Polyimide Networks. *J. Am. Chem. Soc.* **2008**, *130*, 14054–14055.
4. Weigelt, S.; Busse, C.; Bombis, C.; Knudsen, M. M.; Gothelf, K. V.; Laegsgaard, E.; Besenbacher, F.; Linderoth, T. R. Surface Synthesis of 2D Branched Polymer Nanostructures. *Angew. Chem., Int. Ed.* **2008**, *47*, 4406–4410.
5. Bieri, M.; Nguyen, M.-T.; Gröning, O.; Cai, J.; Treier, M.; Aït-Mansour, K.; Ruffieux, P.; Pignedoli, C. A.; Passerone, D.; Kastler, M.; Müllen, K.; Fasel, R., Two-Dimensional Polymer Formation on Surfaces: Insight into the Roles of Precursor Mobility and Reactivity. *J. Am. Chem. Soc.* **2010**, *132*, 16669–16676.
6. Miura, A.; De Feyter, S.; Abdel-Mottaleb, M. M. S.; Gesquiere, A.; Grim, P. C. M.; Moessner, G.; Sieffert, M.; Klapper, M.; Müllen, K.; De Schryver, F. C. Light- and STM-Tip-Induced Formation of One-Dimensional and Two-Dimensional Organic Nanostructures. *Langmuir* **2003**, *19*, 6474–6482.
7. Lipton-Duffin, J. A.; Ivasenko, O.; Perepichka, D. F.; Rosei, F. Synthesis of Polyphenylene Molecular Wires by Surface-Confined Polymerization. *Small* **2009**, *5*, 592–597.
8. Lafferentz, L.; Eberhardt, V.; Dri, C.; Africh, C.; Comelli, G.; Esch, F.; Hecht, S.; Grill, L. Controlling On-Surface Polymerization by Hierarchical and Substrate-Directed Growth. *Nat. Chem.* **2012**, *4*, 215–220.
9. Cai, J.; Ruffieux, P.; Jaafar, R.; Bieri, M.; Braun, T.; Blankenburg, S.; Muoth, M.; Seitsonen, A. P.; Saleh, M.; Feng, X.; Müllen, K.; Fasel, R. Atomically Precise Bottom-Up Fabrication of Graphene Nanoribbons. *Nature* **2010**, *466*, 470–473.
10. Yang, X.; Dou, X.; Rouhanipour, A.; Zhi, L.; Räder, H. J.; Müllen, K. Two-Dimensional Graphene Nanoribbons. *J. Am. Chem. Soc.* **2008**, *130*, 4216–4217.
11. Hla, S. W.; Bartels, L.; Meyer, G.; Rieder, K. H. Inducing All Steps of a Chemical Reaction with the Scanning Tunneling Microscope Tip: Towards Single Molecule Engineering. *Phys. Rev. Lett.* **2000**, *85*, 2777–2780.
12. Blunt, M. O.; Russell, J. C.; Champness, N. R.; Beton, P. H. Templating Molecular Adsorption Using a Covalent Organic Framework. *Chem. Commun.* **2010**, *46*, 7157–7159.
13. Grill, L.; Dyer, M.; Lafferentz, L.; Persson, M.; Peters, M. V.; Hecht, S. Nano-Architectures by Covalent Assembly of Molecular Building Blocks. *Nat. Nanotechnol.* **2007**, *2*, 687–691.
14. Gutzler, R.; Walch, H.; Eder, G.; Kloft, S.; Heckl, W. M.; Lackinger, M. Surface Mediated Synthesis of 2D Covalent Organic Frameworks: 1,3,5-Tris(4-bromophenyl)benzene on Graphite(001), Cu(111), and Ag(110). *Chem. Commun.* **2009**, 4456–4458.
15. Xi, M.; Bent, B. E. Mechanisms of the Ullmann Coupling Reaction in Adsorbed Monolayers. *J. Am. Chem. Soc.* **1993**, *115*, 7426–7433.
16. Lackinger, M.; Heckl, W. M. A STM Perspective on Covalent Intermolecular Coupling Reactions on Surfaces. *J. Phys. D: Appl. Phys.* **2011**, *44*, 464011.
17. Tanoue, R.; Higuchi, R.; Enoki, N.; Miyasato, Y.; Uemura, S.; Kimizuka, N.; Stieg, A. Z.; Gimzewski, J. K.; Kunitake, M. Thermodynamically Controlled Self-Assembly of Covalent Nanoarchitectures in Aqueous Solution. *ACS Nano* **2011**, *5*, 3923–3929.
18. Côté, A. P.; El-Kaderi, H. M.; Furukawa, H.; Hunt, J. R.; Yaghi, O. M. Reticular Synthesis of Microporous and Mesoporous 2D Covalent Organic Frameworks. *J. Am. Chem. Soc.* **2007**, *129*, 12914–12915.
19. Dienstmaier, J. F.; Gigler, A. M.; Goetz, A. J.; Knochel, P.; Bein, T.; Lyapin, A.; Reichlmaier, S.; Heckl, W. M.; Lackinger, M. Synthesis of Well-Ordered COF Monolayers: Surface Growth of Nanocrystalline Precursors *versus* Direct On-Surface Polycondensation. *ACS Nano* **2011**, *5*, 9737–9745.
20. Côté, A. P.; Benin, A. I.; Ockwig, N. W.; O'Keeffe, M.; Matzger, A. J.; Yaghi, O. M. Porous, Crystalline, Covalent Organic Frameworks. *Science* **2005**, *310*, 1166–1170.
21. Han, S. S.; Furukawa, H.; Yaghi, O. M.; Goddard, W. A. Covalent Organic Frameworks as Exceptional Hydrogen Storage Materials. *J. Am. Chem. Soc.* **2008**, *130*, 11580–11581.
22. Guan, C.-Z.; Wang, D.; Wan, L.-J. Construction and Repair of Highly Ordered 2D Covalent Networks by Chemical Equilibrium Regulation. *Chem. Commun.* **2012**, *48*, 2943–2945.
23. Xie, R. S.; Song, Y. H.; Wan, L. L.; Yuan, H. Z.; Li, P. C.; Xiao, X. P.; Liu, L.; Ye, S. H.; Lei, S. B.; Wang, L. Two-Dimensional Polymerization and Reaction at the Solid/Liquid Interface: Scanning Tunneling Microscopy Study. *Anal. Sci.* **2011**, *27*, 129–138.
24. Sakaguchi, H.; Matsumura, H.; Gong, H. Electrochemical Epitaxial Polymerization of Single-Molecular Wires. *Nat. Mater.* **2004**, *3*, 551–557.
25. Russell, J. C.; Blunt, M. O.; Garfitt, J. M.; Scurr, D. J.; Alexander, M.; Champness, N. R.; Beton, P. H. Dimerization of Tri(4-bromophenyl)benzene by Aryl-Aryl Coupling from Solution on a Gold Surface. *J. Am. Chem. Soc.* **2011**, *133*, 4220–4223.
26. Meyer, R.; Lemire, C.; Shaikhutdinov, S.; Freund, H. Surface Chemistry of Catalysis by Gold. *Gold Bull. (Geneva)* **2004**, *37*, 72–124.
27. Schlögl, S.; Heckl, W. M.; Lackinger, M. On-Surface Radical Addition of Triply Iodinated Monomers on Au(111) - The Influence of Monomer Size and Thermal Post-Processing. *Surf. Sci.* **2012**, *606*, 999–1004.
28. Blunt, M. O.; Russell, J. C.; Gimenez-Lopez, M. D.; Taleb, N.; Lin, X. L.; Schröder, M.; Champness, N. R.; Beton, P. H. Guest-Induced Growth of a Surface-Based Supramolecular Bilayer. *Nat. Chem.* **2011**, *3*, 74–78.
29. Walch, H.; Gutzler, R.; Sirtl, T.; Eder, G.; Lackinger, M. Material- and Orientation-Dependent Reactivity for Heterogeneously Catalyzed Carbon−Bromine Bond Homolysis. *J. Phys. Chem. C* **2010**, *114*, 12604–12609.
30. Gutzler, R.; Ivasenko, O.; Fu, C.; Brusso, J. L.; Rosei, F.; Perepichka, D. F. Halogen Bonds as Stabilizing Interactions

in a Chiral Self-Assembled Molecular Monolayer. *Chem. Commun.* **2011**, *47*, 9453–9455.
31. Sakaguchi, H.; Matsumura, H.; Gong, H.; Abouelwafa, A. M. Direct Visualization of the Formation of Single-Molecule Conjugated Copolymers. *Science* **2005**, *310*, 1002–1006.
32. Lapitan, L. D. S.; Tongol, B. J. V.; Yau, S. L. *In Situ* Scanning Tunneling Microscopy Imaging of Electropolymerized Poly(3,4-Ethylenedioxythiophene) on an Iodine-Modified Au(111) Single Crystal Electrode. *Electrochim. Acta* **2012**, *62*, 433–440.
33. Huang, L.; Zeppenfeld, P.; Horch, S.; Comsa, G. Determination of Iodine Adlayer Structures on Au(111) by Scanning Tunneling Microscopy. *J. Chem. Phys.* **1997**, *107*, 585–591.
34. Hla, S. W.; Rieder, K. H. STM Control of Chemical Reactions: Single-Molecule Synthesis. *Annu. Rev. Phys. Chem.* **2003**, *54*, 307–330.
35. *Practical Surface Analysis: Auger and X-ray Photoelectron Spectroscopy*, 2nd ed.; John Wiley & Sons: Chichester, U.K., 1990; Vol. 1.
36. Syomin, D.; Koel, B. E. Adsorption of Iodobenzene (C_6H_5I) on Au(111) Surfaces and Production of Biphenyl (C_6H_5-C_6H_5). *Surf. Sci.* **2001**, *490*, 265–273.
37. McMillen, D. F.; Golden, D. M. Hydrocarbon Bond Dissociation Energies. *Annu. Rev. Phys. Chem.* **1982**, *33*, 493–532.
38. Migani, A.; Illas, F. A Systematic Study of the Structure and Bonding of Halogens on Low-Index Transition Metal Surfaces. *J. Phys. Chem. B* **2006**, *110*, 11894–11906.